

# AST 383 Nucleosynthesis: Assignment 5

---

Attempt 2 of the 4 questions  
Due Thursday, March 24

1. A fundamental requirement of the cold CNO-cycles is that the unstable nuclides such as  $^{13}\text{N}$  beta-decay rather than experience proton capture.

For the intermediate nuclide  $^{13}\text{N}$  in the CN01 cycle show that beta-decay is much more likely than proton capture in the core of the attached model 10 solar mass star.

Beta-decay half-lives are given by Iliadis on page 370. For  $^{13}\text{N}$  the half-life is 9.97 minutes.

Take the reaction rate for  $^{13}\text{N}(p, \gamma) ^{14}\text{O}$  from the NACRE II compilation -----  
<http://www.astro.ulb.ac.be/nacreii/index.html?individualreaction.html>

2. Again with reaction rates from NACRE II calculate the equilibrium abundance ratios  $^{12}\text{C}/^{13}\text{C}$ ,  $^{12}\text{C}/^{14}\text{N}$  and  $^{14}\text{N}/^{15}\text{N}$  for these participants in the CN01 cycles for temperatures  $T_6 = 10(10)50$  K. Also estimate approximate uncertainties for each of the three ratios.
3. The figure below from Dearborn, Eggleton and Schramm (1976, ApJ, 203, 455) shows the interior composition of a 1 solar mass star near the end of its main-sequence evolution.

Explain qualitatively in terms of operation of the pp-chains and the CN0 cycles the changes in composition from surface ( $M(R)=1$ ) to the core ( $M(R)=0$ ).

Discuss why the enrichment of  $^3\text{He}$  is relevant to the interpretation of measurements of  $^3\text{He}^+/\text{H}$  from galactic H II regions as an indicator of  $^3\text{He}$  synthesis by the Big Bang.

4. Describe the principal factors controlling the subsurface increase in the  $^3\text{He}$  mass fraction in the Dearborn et al. figure, the origin of the broad peak and the sharp fall into the core. Using the attached model of a solar mass star and NACRE II rates estimate the  $^3\text{He}$  mass fraction between  $M(R) = 0.25$  and  $0.75$  and compare your results with the profile in the figure.

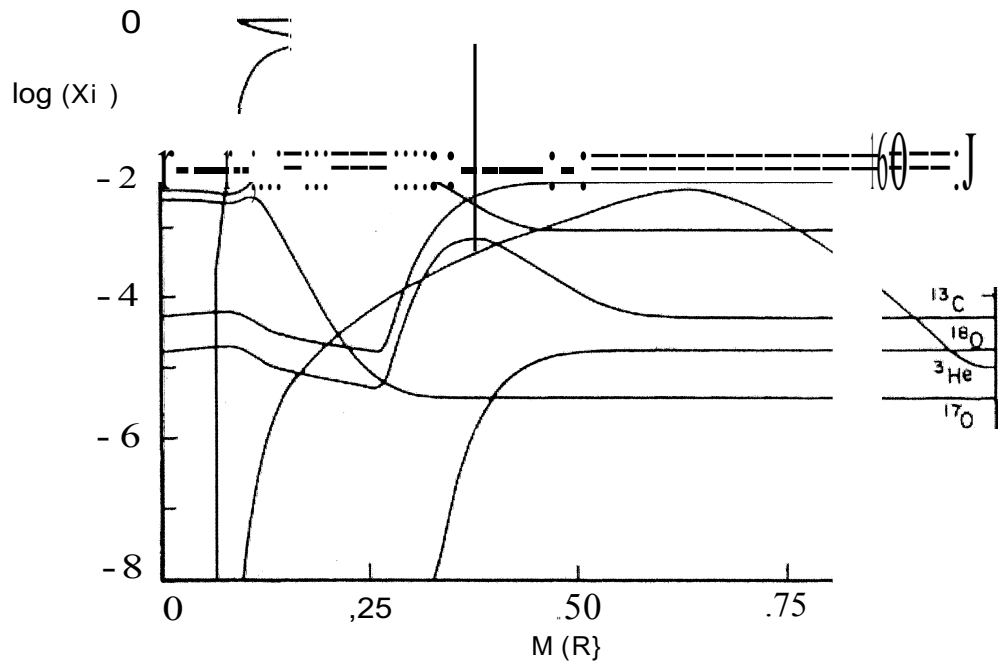


FIG. 1.—Composition of a  $1 M_{\odot}$  star near the end of its main-sequence evolution

Table 9.3(c) (continued).

$r/R^a$	$M_r/M^b$	$L_r/L^c$	$\log(\rho)$	$\log(P)$	$\log[T(K)]$	$\kappa^d$
0.92	0.999	1.000	-1.463	12.392	5.733	241.88*
0.95	1.000	1.000	-1.820	11.785	5.488	965.14*
0.97	1.000	1.000	-2.123	11.285	5.297	
0.98	1.000	1.000	-2.753	10.285	4.947	
1.00	1.000	1.000	-6.273	5.285	3.754	0.33

Notes:

<sup>a</sup>  $R = 6.07 \cdot 10^{10}$  cm

<sup>b</sup>  $M = 1.0 \cdot 1.99 \cdot 10^{33}$  gm

<sup>c</sup>  $L = 2.72 \cdot 10^{33}$  ergs/sec

$P$  and  $\rho$  in cgs units.

<sup>d</sup> Opacity in  $\text{cm}^2/\text{gm}$ . The asterisk means the stellar temperature gradient is adiabatic.

Age = 0.042 Gyr,  $X = 0.702$ ,  $Z = 0.019$ .

Table 9.3(c). Model of a 1 Solar Mass Main-Sequence Star

$r/R^e$	$M_r/M^b$	$L_r/L^c$	$\log(\rho)$	$\log(P)$	$\log[T(K)]$	$\kappa^d$
0.03	0.001	0.021	1.891	17.158	7.133	1.46*
0.04	0.002	0.046	1.888	17.151	7.131	1.47*
0.06	0.008	0.135	1.876	17.132	7.123	1.51*
0.08	0.018	0.257	1.860	17.106	7.113	1.55*
0.10	0.035	0.390	1.839	17.071	7.099	1.61*
0.12	0.058	0.510	1.814	17.029	7.082	1.69*
0.14	0.088	0.642	1.783	16.978	7.062	1.79
0.16	0.126	0.769	1.746	16.919	7.041	1.90
0.18	0.170	0.868	1.702	16.853	7.018	2.03
0.20	0.219	0.931	1.653	16.780	6.993	2.17
0.22	0.272	0.967	1.597	16.698	6.968	2.33
0.24	0.327	0.987	1.536	16.612	6.943	2.50
0.26	0.385	0.999	1.468	16.518	6.918	2.68
0.28	0.442	1.005	1.395	16.419	6.892	2.88
0.30	0.496	1.008	1.319	16.317	6.868	3.10
0.32	0.550	1.008	1.234	16.207	6.842	3.33
0.34	0.596	1.008	1.155	16.104	6.819	3.57
0.36	0.646	1.007	1.059	15.981	6.793	3.86
0.38	0.684	1.006	0.976	15.877	6.771	4.14
0.40	0.725	1.004	0.878	15.753	6.746	4.53
0.42	0.759	1.003	0.784	15.637	6.724	4.93
0.44	0.785	1.002	0.703	15.536	6.704	5.31
0.46	0.813	1.001	0.608	15.418	6.682	5.80
0.48	0.832	1.001	0.536	15.329	6.665	6.20
0.51	0.860	1.000	0.415	15.180	6.637	7.04
0.53	0.876	1.000	0.335	15.081	6.618	7.65
0.54	0.891	1.000	0.254	14.981	6.599	8.30
0.56	0.904	0.999	0.174	14.881	6.579	9.00
0.58	0.916	0.999	0.094	14.781	6.559	9.75
0.60	0.927	0.999	0.014	14.681	6.539	10.56
0.63	0.940	0.999	-0.104	14.531	6.508	11.72
0.65	0.948	0.999	-0.182	14.432	6.486	12.58
0.67	0.955	0.999	-0.259	14.332	6.464	13.58
0.69	0.962	0.999	-0.336	14.232	6.440	14.81
0.71	0.967	0.999	-0.409	14.133	6.415	16.44
0.72	0.972	0.999	-0.479	14.033	6.385	18.85
0.74	0.976	0.999	-0.539	13.939	6.351	22.62*
0.77	0.981	1.000	-0.629	13.790	6.291	31.05*
0.78	0.984	1.000	-0.688	13.690	6.251	37.75*
0.80	0.988	1.000	-0.778	13.540	6.191	47.30*
0.83	0.991	1.000	-0.868	13.390	6.132	58.07*
0.84	0.993	1.000	-0.958	13.241	6.072	70.94*
0.86	0.995	1.000	-1.048	13.091	6.012	85.54*
0.88	0.997	1.000	-1.168	12.891	5.932	110.36*
0.90	0.998	1.000	-1.316	12.641	5.832	158.13*

